REPORT DOCUMENTATION PAGE

Form Approved
OMB No. 0704-0188

1. REPORT DATE *(DD-MM-YYYY)*	**2. REPORT TYPE**	**3. DATES COVERED** *(From - To)*
21-08-2007	Technical Paper	

4. TITLE AND SUBTITLE

Effects of Helicon Wave Propagation Based on a Conical Antenna Design: Part I (Preprint)

5a. CONTRACT NUMBER

5b. GRANT NUMBER

5c. PROGRAM ELEMENT NUMBER

6. AUTHOR(S)
Michael P. Reilly and George H. Miley (Univ. of Illinois); David E. Kirtley (Univ of Mich); Justin Koo and William A. Hargus, Jr. (AFRL/PRSS)

5d. PROJECT NUMBER

5e. TASK NUMBER
23080535

5f. WORK UNIT NUMBER

7. PERFORMING ORGANIZATION NAME(S) AND ADDRESS(ES)

Air Force Research Laboratory (AFMC)
AFRL/PRSS
1 Ara Drive
Edwards AFB CA 93524-7013

8. PERFORMING ORGANIZATION REPORT NUMBER

AFRL-PR-ED-TP-2007-388

9. SPONSORING / MONITORING AGENCY NAME(S) AND ADDRESS(ES)

Air Force Research Laboratory (AFMC)
AFRL/PRS
5 Pollux Drive
Edwards AFB CA 93524-7048

10. SPONSOR/MONITOR'S ACRONYM(S)

11. SPONSOR/MONITOR'S NUMBER(S)
AFRL-PR-ED-TP-2007-388

12. DISTRIBUTION / AVAILABILITY STATEMENT

Approved for public release; distribution unlimited (PA #07323A).

13. SUPPLEMENTARY NOTES
For presentation at the 30th International Electric Propulsion Conference (2007 IEPC), Florence Italy, 17-20 Sep 2007. IEPC-2007-196.

14. ABSTRACT

The requirement for a highly efficient plasma source that can operate in an electric propulsion capacity has led to renewed research on helicons. Helicons have long been known to be a highly efficient (>90%) and high density (>1013 cm-3) method to generate plasma. It has not been until recently though, that these sources have been given interest by the propulsion community. Much recent research toward this end has focused on detachment of ions from the magnetic field lines which can be as great as a few hundred Gauss. Investigations to date have shown that this may be possible through ambipolar effects or acceleration through a double layer. Preliminary investigations suggest electrons that are generated near the diverging section of the axial magnetic field will enhance the ambipolar acceleration of ions out of the device. Toward this end, a radio frequency (RF) antenna that propagates a wave toward the converging section of the device (diverging section of the magnetic field) will dictate where the bulk of the RF energy is absorbed. This has led to the design of a conical antenna. Preliminary work based on a uniform density model suggest that at smaller radii there is an increase in electron density and that there are further ways to control the density and temperature based on considerations such as pressure, frequency, and antenna length. The focus of this investigation will be to observe and compare the differences in the wave fields (Br, Bθ, Bz) between a traditional cylindrical helicon and that of a conical helicon.

15. SUBJECT TERMS

16. SECURITY CLASSIFICATION OF:			**17. LIMITATION OF ABSTRACT**	**18. NUMBER OF PAGES**	**19a. NAME OF RESPONSIBLE PERSON**
					Dr. William A. Hargus, Jr.
a. REPORT	**b. ABSTRACT**	**c. THIS PAGE**	SAR	32	**19b. TELEPHONE NUMBER** *(include area code)*
Unclassified	**Unclassified**	**Unclassified**			N/A

Effects of Helicon Wave Propagation Based on a Conical Antenna Design: Part I

IEPC-2007-196

Presented at the 30th International Electric Propulsion Conference, Florence, Italy
September 17-20, 2007

Michael P. Reilly* and George H. Miley†
University of Illinois @ Urbana-Champaign, Urbana, IL. 61801, United States of America

David E. Kirtley‡
University of Michigan, Ann Arbor, MI. 48109, United States of America

and

William A. Hargus, Jr§
Air Force Research Laboratory, Edwards AFB, CA. 93524 United States of America

Abstract

The requirement for a highly efficient plasma source that can operate in an electric propulsion capacity has led to renewed research on helicons. Helicons have long been known to be a highly efficient (>90%) and high density (>10^{13} cm^{-3}) method to generate plasma. It has not been until recently though, that these sources have been given interest by the propulsion community. Much recent research toward this end has focused on detachment of ions from the magnetic field lines which can be as great as a few hundred Gauss. Investigations to date have shown that this may be possible through ambipolar effects or acceleration through a double layer. Preliminary investigations suggest electrons that are generated near the diverging section of the axial magnetic field will enhance the ambipolar acceleration of ions out of the device. Toward this end, a radio frequency (RF) antenna that propagates a wave toward the converging section of the device (diverging section of the magnetic field) will dictate where the bulk of the RF energy is absorbed. This has led to the design of a conical antenna. Preliminary work based on a uniform density model suggest that at smaller radii there is an increase in electron density and that there are further ways to control the density and temperature based on considerations such as pressure, frequency, and antenna length. The focus of this investigation will be to observe and compare the differences in the wave fields (B_r, B_θ, B_z) between a traditional cylindrical helicon and that of a conical helicon.

* Graduate Student, Nuclear, Plasma, and Radiological Engineering, mreilly@uiuc.edu
† Professor and Laboratory Director, Nuclear, Plasma, and Radiological Engineering, ghmiley@uiuc.edu
‡ Graduate Student, Aerospace Engineering, dkirtley@umich.edu
§ Research Scientist, Spacecraft Branch, AFRL/PRSS, william.hargus.ctr@edwards.af.mil

Nomenclature

a = fixed radius
B_0 = static magnetic field
B_r = radial component of magnetic field
B_θ = azimuthal component of magnetic field
B_z = axial component of magnetic field
E = electric field ω_c = cyclotron frequency
e = electric charge ω_p = plasma frequency
f = driving frequency
g = generic function
i = imaginary number
J_m = Bessel function
j = current density
k = wave number
$\mathbf{k}$ = wave vector
m = mode number
n = density (plasma + neutral)
n_0 = plasma density
n_e = electron density
$P_l,^m$ = associated Legendre polynomial
r = radius
t = time
$Y_l,^m$ = spherical harmonic
x,y,z = Cartesian units
μ_0 = permeability of free space
ϕ = spherical angle
θ = cylindrical/spherical angle
θ_{wall} = fixed angle of cone
ω = driving frequency

I. Introduction

The term 'helicon' was first used in 1960 by Aigrain [1], to describe waves that propagate in the presence of a magnetic field for the frequencies between the ion and electron cyclotron frequencies. Helicon waves are a subclass of whistler waves which were first investigated by Storey in the 1950's [2]. Whistler waves are right-handed circularly polarized waves that propagate in free space differing from helicons in two main regards: (1) helicons are of such a lower frequency than whistler waves that the electron gyrations (being so much faster) may be neglected and (2) helicons propagate in a bounded system [3], specific to this study, a cylindrical or conical boundary. Helicon waves were initially studied in metals and semiconductors by Libchaber [4] and Rose [5] in the early 1960's who observed the wave propagation at frequencies much less than the electron cyclotron frequency and whose wave vector **k** was parallel to the magnetic field. Soon afterwards, helicons were observed in gaseous plasma by Lehane and Thoneman [6], Kuckes [7], and Nyack and Christiansen [8] who all observed right-handed circularly polarized waves in a laboratory experiment. The experiments were run from power levels of several hundred watts to three kilo-watts while a dc solenoidal field of several hundred Gauss was applied. All three found comparisons to agree well with the theory of plasma wave propagation in an insulated cylinder for a uniform plasma profile originally derived by Klozenberg, McNamara, and Thoneman [9] (KMT theory). However, the experiments were limited in scope by the diagnostics and equipment at hand and it wasn't until the 1970's when Boswell presented his work on waves in gaseous plasma [10-13] and Chen [3, 14-27] began to investigate helicons that much experimental data began to be produced. Thus, the great majority of theory and experimental data that is relevant to this study was done by Boswell, Charles, and Chen. Specifically, the resonant absorption of waves in plasma at or near the lower hybrid frequency as well as downstream density peaks and most recently double layers is what this work will ultimately investigate.

II. Cylindrical Wave Fields

The description of helicon waves follows the analysis of Chen and others where the basic equation to be solved is the simplified Ohm's law

$$ne\overline{E} = \overline{j} \times \overline{B_0} \tag{1.1}$$

where the static applied magnetic field is $\overline{B_0} = B_0 \hat{z}$ and we use Maxwell's equations

$$\nabla \times \overline{E} = -\frac{\partial \overline{B}}{\partial t} \tag{1.2}$$

$$\nabla \times \overline{B} = \mu_0 \overline{j} \tag{1.3}$$

$$\nabla \cdot \overline{B} = 0 \tag{1.4}$$

$$\nabla \cdot \overline{j} = 0 \tag{1.5}$$

with perturbations of the form $\exp i(m\theta + kz - \omega t)$ to obtain

$$\overline{B} = \left(\frac{\omega}{k} \frac{\mu_0 e n_0}{B_0} \right)^{-1} \nabla \times \overline{B} \tag{1.6}$$

where we let

$$\alpha \equiv \frac{\omega}{k} \frac{\mu_0 e n_0}{B_0} = \frac{\omega}{k} \frac{\omega_p^2}{\omega_c c^2} \tag{1.7}$$

And equation (1.6) then becomes

$$\nabla \times \overline{B} = \alpha \overline{B} \tag{1.8}$$

and finally taking the curl of equation (1.8) yields

$$\nabla^2 \overline{B} + \alpha^2 \overline{B} = 0 \tag{1.9}$$

Writing this in cylindrical coordinates for the z-component gives

$$B_z'' + \frac{1}{r} B_z' + \left(T^2 - \frac{m^2}{r^2} \right) B_z = 0 \tag{1.10}$$

where $T^2 = \alpha^2 + k^2$

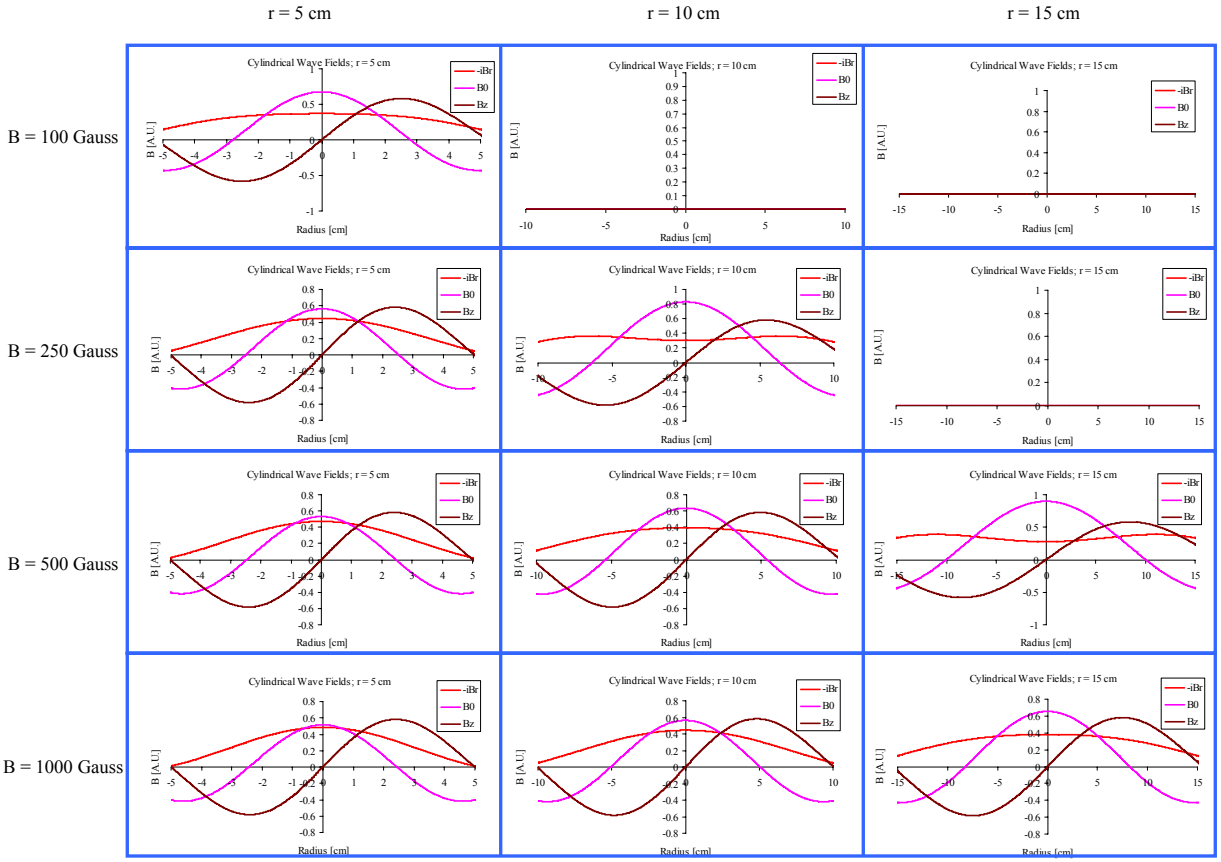

Figure 1. Evolution of Cylindrical Helicon Wave Fields with Increasing Applied Magnetic Field.

There must be a finite solution at $r=0 \rightarrow J_m(Tr)$, so that

$$B_z = C_3 J_m(Tr) \tag{1.11}$$

The r and θ components are then obtained from equation (1.8)

$$\frac{im}{r} B_z - ikB_\theta = \alpha B_r \tag{1.12}$$

$$ikB_r - B_z^{'} = \alpha B_\theta \tag{1.13}$$

These can then be algebraically manipulated into solving for the r and θ components of the magnetic field in terms of Bessel functions J_m

$$B_r = \frac{iC_3}{T^2}\left(\frac{m}{r}\alpha J_m - kJ_m^{'}\right) \tag{1.14}$$

$$B_\theta = \frac{C_3}{T^2}\left(\frac{m}{r}kJ_m + \alpha J_m^{'}\right) \tag{1.15}$$

We can now analyze what the field structure should look like given some basic input parameters. For the cases considered here, we assume a uniform electron density of 10^{12} cm^{-3}, 13.56 MHz driving frequency, and an m=+1 helical antenna. We take a look at three separate cases of varying radial size, namely, cylinders of 5, 10, and 15 cm radii. The results are indicated in Figure 1. Here we find that for the density selected helicon waves will not propagate at lower magnetic fields if the radius is too large. At 100 Gauss external field, only the 5 cm radius geometry will support helicon waves. It is not until the applied field reaches 250 Gauss that the 10 cm geometry will support wave propagation and until about 500 Gauss that the 15 cm geometry will support helicon waves. Additionally, once the applied external magnetic field is great enough to allow helicon wave propagation, further increase in applied field does not change the structure. At least not until more input power is available. A higher level of input power will raise the electron density and the helicon wave field will start to dissipate until a higher magnetic field is applied. Clearly, there is a delicate balance between the input power and applied magnetic field necessary to sustain helicon wave propagation.

Being able to address the profile of the radial magnetic field is what differentiates a purely inductive discharge from a helicon discharge. So if we are to investigate different geometries such as the conical one proposed here, we will need to perform a similar analysis to that done in cylindrical geometry to look at the new radial profiles.

III. Spherical Wave Expansion for Conical Geometry

In cylindrical coordinates, helicon waves are described by perturbations of the form,

$$\exp i(m\theta + kz - \omega t) \tag{2.1}$$

where the coordinate system used is $\hat{r} + \hat{\theta} + \hat{z}$. This represents waves traveling in the +z direction in time and rotating either clockwise (m>0) or counterclockwise (m<0) with respect to θ. However, when examining helicon waves in a spherical coordinate system to describe wave propagation in a cone, the perturbations must take a different form. To begin the analysis we assume spherical perturbations are of the form

$$\exp i(m\phi + kr - \omega t) \tag{2.2}$$

where the coordinate system is $\hat{r} + \hat{\theta} + \hat{\phi}$. This represents waves traveling in the r direction in time and rotating either clockwise (m>0) or counterclockwise (m<0) with respect to ϕ. The perturbations described here assume wave propagation in the $\hat{r}$ direction where the cone wall is given by a constant $\theta = \theta_{wall}$ from the x-axis. The situation is illustrated below in Figure 2.

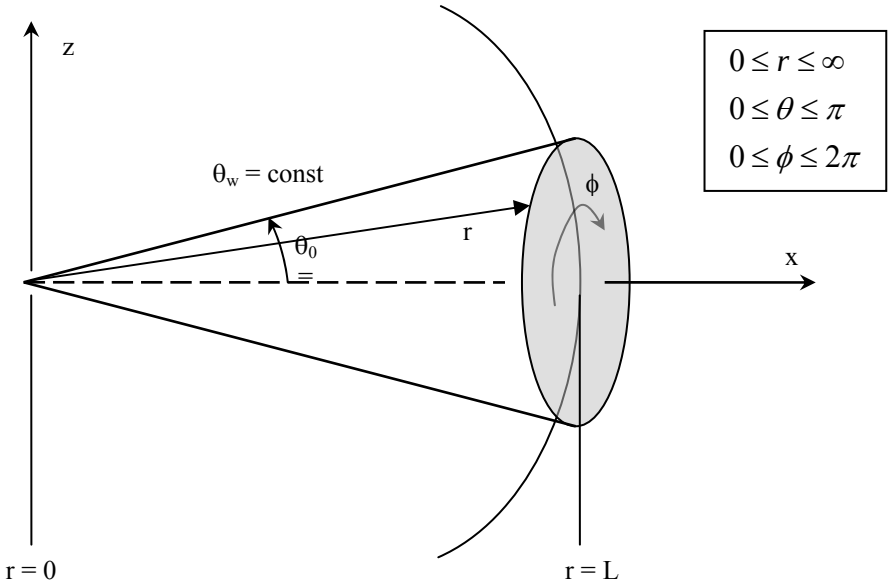

Figure 2. Coordinate Axis for Analyzing Conical Antenna Design.

When utilizing a cylindrical coordinate system to study helicon waves, the system inherently allows for the simplicity of applying a constant magnetic field B_0 in the z-direction; or the direction of wave propagation. However, when analyzing wave propagation in spherical geometry, a constant magnetic field in the Cartesian or cylindrical z-direction now must be given in terms of the different unit vectors; $\hat{r}, \hat{\theta}, \hat{\phi}$. The system described above is shown in Figure 3 but now includes the applied magnetic field in the Cartesian/cylindrical +z-direction. The objective is to describe the magnetic field in terms of the spherical unit vectors.

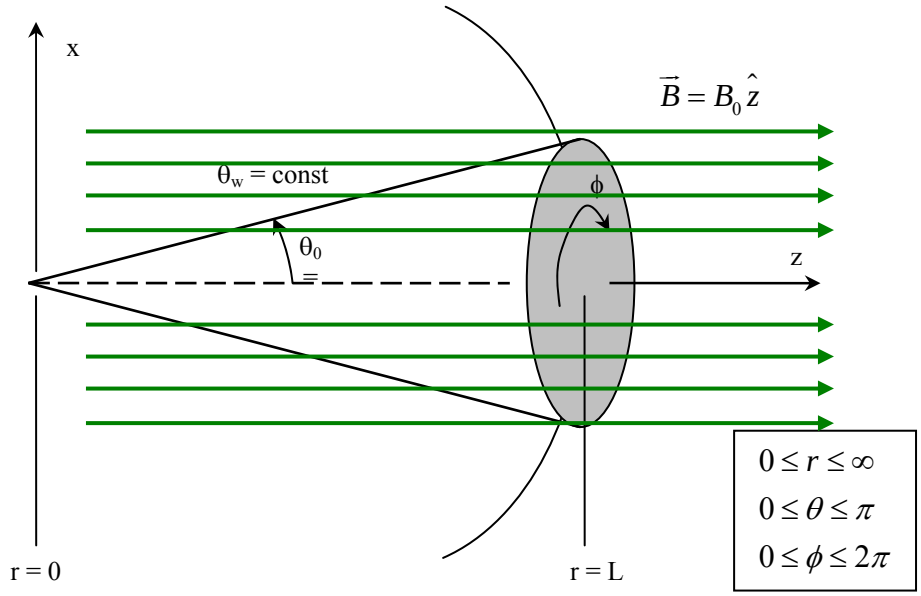

Figure 3. Direction of Applied Magnetic Field with Spherical Coordinates.

To describe the unit vectors in the z-direction, we must first write the spherical unit vectors in terms of their cartesian counterparts,

$$\begin{aligned}\hat{r} &= \sin\theta\cos\phi\hat{x} + \sin\theta\sin\phi\hat{y} + \cos\theta\hat{z} \\ \hat{\theta} &= \cos\theta\cos\phi\hat{x} + \cos\theta\sin\phi\hat{y} - \sin\theta\hat{z} \\ \hat{\phi} &= -\sin\phi\hat{x} + \cos\phi\hat{y}\end{aligned} \tag{2.3}$$

These are the normalized spherical unit vectors. We can now algebraically manipulate the above 3 equations and solve for the unit vector in the z-direction in terms of $\hat{r}, \hat{\theta}, \hat{\phi}$ which yields

$$\hat{z} = \cos\theta\hat{r} - \sin\theta\hat{\theta} \tag{2.4}$$

Therefore, when describing the static magnetic field applied in the z-direction, we can relate the different coordinate systems by,

$$\vec{B} = B_0\hat{z} = B_0(\cos\theta\hat{r} - \sin\theta\hat{\theta}) \tag{2.5}$$

We can now begin to describe the wave propagation in spherical coordinates beginning with Ohm's law as in equation (1.1),

$$ne\vec{E} = \vec{j} \times \vec{B_0} \tag{2.6}$$

where $\boldsymbol{B_0}$ is given above in equation (2.5). Again we make use of Maxwell's equations

$$\nabla \times \vec{E} = -\frac{\partial \vec{B}}{\partial t} \tag{2.7}$$

$$\nabla \times \vec{B} = \mu_0 \vec{j} \tag{2.8}$$

$$\nabla \cdot \vec{B} = 0 \tag{2.9}$$

$$\nabla \cdot \vec{j} = 0 \tag{2.10}$$

and perturbations given by $\exp i(m\phi + kr - \omega t)$ so that equation (2.7) becomes

$$\nabla \times \vec{E} = i\omega\vec{B} \tag{2.11}$$

Taking the curl of equation (2.6) to obtain

$$\nabla \times \vec{E} = \frac{\nabla \times \vec{j} \times \vec{B_0}}{ne} = \frac{(\vec{B_0}\cdot\nabla)\vec{j} - (\vec{j}\cdot\nabla)\vec{B_0} + \vec{j}(\nabla\cdot\vec{B_0}) - \vec{B_0}(\nabla\cdot\vec{j})}{ne} \tag{2.12}$$

The third and fourth terms of equation (2.12) are zero as a result of Maxwell's equations (2.9) and(2.10). Additionally the second term is zero because the applied magnetic field is constant in all directions. If we now equate the left hand sides of equation (2.11) and (2.12) we arrive at

$$i\omega\vec{B} = \frac{(\vec{B_0}\cdot\nabla)\vec{j}}{ne} \tag{2.13}$$

In terms of the wave perturbations, ***j*** is similarly defined as

$$\vec{j} = j\exp i(m\phi + kr - \omega t) \tag{2.14}$$

If we now expand equation(2.13), we obtain,

$$i\omega\vec{B} = \frac{1}{ne}\left\{\left[\left(B_0\cos\theta\hat{r} - B_0\sin\theta\hat{\theta}\right)\cdot\left(\frac{\partial}{\partial r}\hat{r} + \frac{1}{r}\frac{\partial}{\partial\theta}\hat{\theta} + \frac{1}{r\sin\theta}\frac{\partial}{\partial\phi}\hat{\phi}\right)\right]\vec{j}\right\} \tag{2.15}$$

which upon simplifying the inner product becomes,

$$i\omega\vec{B} = \frac{1}{ne}\left\{\left(B_0\cos\theta\frac{\partial}{\partial r} - B_0\sin\theta\frac{1}{r}\frac{\partial}{\partial\theta}\hat{\theta}\right)\vec{j}\right\} \tag{2.16}$$

Inserting equation (2.14) for ***j*** into equation (2.16)

$$i\omega\vec{B} = \frac{1}{ne}\left\{\left(B_0\cos\theta\frac{\partial}{\partial r} - B_0\sin\theta\frac{1}{r}\frac{\partial}{\partial\theta}\hat{\theta}\right)j\exp i(m\phi + kr - \omega t)\right\} \tag{2.17}$$

However, the partial derivative with respect to θ is zero because the current term is assumed to be constant across the radial arc from $-\theta_{wall}$ to $+\theta_{wall}$.

Note: This assumption does not include a perturbation in the θ-direction. This assumption was based on the helicon wave analysis done in cylindrical geometry where the basic assumption of a uniform density gives rise to plane wave propagation. In spherical coordinates, similar waves are assumed to propagate although the waves are spherical waves of a constant radius '***r***'.

Simplifying equation (2.17) will yield,

$$i\omega\vec{B} = \frac{B_0 ik\cos\theta\left(j\exp i(m\phi + kr - \omega t)\right)}{ne} \tag{2.18}$$

which becomes

$$\vec{B} = \frac{\left(B_0 k\cos\theta\right)\vec{j}}{\omega ne} \tag{2.19}$$

Inserting equation (2.8) for ***j***

$$\vec{B} = \frac{\left(B_0 k\cos\theta\right)}{\mu_0\omega ne}\nabla\times\vec{B} \tag{2.20}$$

If we define the constants in equation (2.20) as

$$\alpha = \frac{\mu_0 \omega n e}{B_0 k} \tag{2.21}$$

Then equation (2.20) becomes

$$\alpha \vec{B} = \left(\cos\theta\right) \nabla \times \vec{B} \tag{2.22}$$

Taking the curl of both sides of equation (2.22)

$$\alpha \nabla \times \vec{B} = \nabla \times \left\{ \left(\cos\theta\right) \nabla \times \vec{B} \right\} \tag{2.23}$$

The analysis becomes further complicated when considering the curl in equation(2.23), there is the additional $\cos\theta$ term. Equation (2.23) then becomes

$$\alpha \nabla \times \vec{B} = \nabla \times \left\{ \begin{array}{r} \dfrac{\cos\theta}{r \sin\theta} \left\{ \dfrac{\partial}{\partial \theta}\left(\sin\theta B_\phi\right) - \dfrac{\partial B_\theta}{\partial \phi} \right\} \hat{r} + \ldots \\ \ldots + \cos\theta \left\{ \dfrac{1}{r \sin\theta} \dfrac{\partial B_r}{\partial \phi} - \dfrac{1}{r} \dfrac{\partial}{\partial r}\left(r B_\phi\right) \right\} \hat{\theta} + \ldots \\ \ldots + \dfrac{\cos\theta}{r} \left\{ \dfrac{\partial}{\partial r}\left(r B_\theta\right) - \dfrac{\partial B_r}{\partial \theta} \right\} \hat{\phi} \end{array} \right\} \tag{2.24}$$

And in order to ultimately arrive at the second order differential equation for the magnetic field structure, the Laplacian in spherical coordinates is needed

$$\nabla^2 = \frac{1}{r^2} \frac{\partial}{\partial r}\left(r^2 \frac{\partial}{\partial r} \right) + \frac{1}{r^2 \sin\theta} \frac{\partial}{\partial \theta}\left(\sin\theta \frac{\partial}{\partial \theta} \right) + \frac{1}{r^2 \sin^2\theta} \frac{\partial^2}{\partial \phi^2} \tag{2.25}$$

For reference, the curl in spherical coordinates is given by

$$\begin{aligned} \nabla \times \vec{B} = & \frac{1}{r \sin\theta} \left\{ \frac{\partial}{\partial \theta}\left(\sin\theta B_\phi\right) - \frac{\partial B_\theta}{\partial \phi} \right\} \hat{r} + \ldots \\ & \ldots + \left\{ \frac{1}{r \sin\theta} \frac{\partial B_r}{\partial \phi} - \frac{1}{r} \frac{\partial}{\partial r}\left(r B_\phi\right) \right\} \hat{\theta} + \frac{1}{r} \left\{ \frac{\partial}{\partial r}\left(r B_\theta\right) - \frac{\partial B_r}{\partial \theta} \right\} \hat{\phi} \end{aligned} \tag{2.26}$$

If we attempt to look at this from a different perspective and assume that because the conical angle we are looking at in the lab is small (~ 4^o), we can approximate ***B*** as

$$\vec{B} = B_0 \hat{z} = B_0 \hat{r} \tag{2.27}$$

We will still assume perturbations of the form $\exp i(m\phi + kr - \omega t)$ and will reconsider the problem beginning with equation (2.13) and expanding such that

$$i\omega\vec{B} = \frac{1}{ne}\left\{\left[\left(B_0\hat{r}\right)\nabla\left(\frac{\partial}{\partial r}\hat{r} + \frac{1}{r}\frac{\partial}{\partial\theta}\hat{\theta} + \frac{1}{r\sin\theta}\frac{\partial}{\partial\phi}\hat{\phi}\right)\right]\vec{j}\right\} \tag{2.28}$$

Substituting equation (2.14) into equation (2.28) yields

$$i\omega\vec{B} = \frac{1}{ne}\left\{B_0\frac{\partial}{\partial r}\left(j\exp i(m\phi + kr - \omega t)\right)\right\} = \frac{B_0 ik}{ne}\vec{j} \tag{2.29}$$

If we now substitute Maxwell's equation (2.8) for ***j*** into equation (2.29) we arrive at

$$\vec{B} = \frac{B_0 k}{\mu_0\omega ne}\nabla\times\vec{B} = \frac{1}{\alpha}\nabla\times\vec{B} \tag{2.30}$$

where α is defined identically as in equation (2.21). Taking the curl of both sides of equation (2.30) where $\nabla\times\left(\nabla\times\vec{B}\right) = \nabla\left(\nabla\cdot\vec{B}\right) - \nabla^2\vec{B}$ where the second term is zero according to Maxwell's equation (2.9). Equation (2.30) then becomes

$$-\nabla^2\vec{B} = \alpha\nabla\times\vec{B} = \alpha^2\vec{B} \tag{2.31}$$

$$\nabla^2\vec{B} + \alpha^2\vec{B} = 0 \tag{2.32}$$

Which is the Helmholtz equation for spherical coordinates and is written

$$\frac{1}{r^2}\frac{\partial}{\partial r}\left(r^2\frac{\partial\vec{B}}{\partial r}\right) + \frac{1}{r^2\sin\theta}\frac{\partial}{\partial\theta}\left(\sin\theta\frac{\partial\vec{B}}{\partial\theta}\right) + \frac{1}{r^2\sin^2\theta}\frac{\partial^2\vec{B}}{\partial\phi^2} + \alpha^2\vec{B} = 0 \tag{2.33}$$

This equation is separable using the approach

$$B(r,\theta,\phi) = R(r)\Theta(\theta)\Phi(\phi) \tag{2.34}$$

When substituting equation (2.34) into equation (2.33) yields

$$\frac{1}{R}\frac{\partial}{\partial r}\left(r^2\frac{\partial\vec{R}}{\partial r}\right) + \alpha^2 r^2 + \frac{1}{\Theta\sin\theta}\frac{\partial}{\partial\theta}\left(\sin\theta\frac{\partial\vec{\Theta}}{\partial\theta}\right) + \frac{1}{\Phi\sin^2\theta}\frac{\partial^2\vec{\Phi}}{\partial\phi^2} = 0 \tag{2.35}$$

We can take the terms that only involve ϕ of the last term in equation (2.35) and set it equal to a constant $-m^2$ we obtain

$$\frac{1}{\Phi}\frac{d^2\vec{\Phi}}{d\phi^2} = -m^2 \tag{2.36}$$

This transforms equation (2.35) such that the last two terms are now a function of θ only and the constant *m*. We can set these terms equal to another constant *-l(l+1)* which will be helpful when solving the radial components. The θ components of equation (2.35) then become

$$\frac{1}{\Theta\sin\theta}\frac{d}{d\theta}\left(\sin\theta\frac{d\vec{\Theta}}{d\theta}\right)+\frac{-m^2}{\sin^2\theta} = -l\left(l+1\right) \tag{2.37}$$

Equation (2.36) has the familiar solution as a simple harmonic oscillator while equation (2.37) is recognized as the associated Legendre equation. The solution to both are given by

$$\Phi\left(\phi\right) = e^{im\phi} \tag{2.38}$$

$$\Theta\left(\theta\right) = P_l^m\left(\cos\theta\right) \tag{2.39}$$

In which *l=0,1,2,…* and *m* runs over the integer values from *–l* to *l*, and $P_l^m\left(\cos\theta\right)$ are the associated Legendre polynomials. If *l* is not an integer, the solution to equation (2.37) diverges for cosθ = 1 or -1 (θ = 0 or π). Often the solutions of Θ and Φ are combined such that

$$\Theta\left(\theta\right)\Phi\left(\phi\right) = P_l^m\left(\cos\theta\right)e^{im\phi} = Y_l^m\left(\theta,\phi\right) \tag{2.40}$$

where $Y_l^m\left(\theta,\phi\right)$ are known as spherical harmonics. Now examining the radial components of equation (2.35) yields

$$\frac{d}{dr}\left(r^2\frac{d\vec{R}}{dr}\right)+\left[\alpha^2r^2-l\left(l+1\right)\right]R = 0 \tag{2.41}$$

Equivalently, this can be written as

$$r^2\frac{d^2\vec{R}}{dr^2}+2r\frac{d\vec{R}}{dr}+\left[\alpha^2r^2-l\left(l+1\right)\right]R = 0 \tag{2.42}$$

Making the appropriate substitution so that

$$R\left(r\right) = \frac{Z\left(r\right)}{\left(\alpha r\right)^{1/2}} \tag{2.43}$$

Transforms equation (2.42) to

$$r^2\frac{d^2\vec{Z}}{dr^2}+r\frac{d\vec{R}}{dr}+\left[\alpha^2r^2-l\left(l+1/2\right)^2\right]Z = 0 \tag{2.44}$$

The solution to this equation is given by the Bessel's function of *l+1/2* order which are $J_{l+1/2}(\alpha r)$ and $N_{l+1/2}(\alpha r)$. Combining these with the original substitution of equation (2.43) yields

$$j_l(\alpha r) = \frac{J_{l+1/2}(\alpha r)}{(\alpha r)^{1/2}} \tag{2.45}$$

which are the spherical Bessel functions of the first kind. The $N_{l+1/2}(\alpha r)$ terms have been dropped to ensure that the solution is finite at the origin. If we now recombine solutions to the spherical Helmholtz equation as defined in equation (2.34) we obtain

$$B(r,\theta,\phi) = \sum_{l=0}^{\infty} \sum_{m=-l}^{l} a_{lm} j_l(\alpha r) Y_l^m(\theta,\phi) \tag{2.46}$$

where a_{lm} are determined by the boundary conditions.

Note: This is of course the simplified version of the traveling spherical waves.
Key assumptions made:

1) Perturbation is of the form $\exp i(m\phi + kr - \omega t)$. We know that this is incorrect because it violates conservation of energy. The energy density stored in the wave is equal to the square of its amplitude. However, the outgoing wave increases its area by a factor of r^2. This would imply that the energy of the wavefront increases as r^2. This cannot be true and we can eliminate this fact by dividing the amplitude by *r* (which divides the energy density by r^2). So the new (correct form) of perturbations to the spherically traveling waves must be

$$g \propto g_0 \frac{\exp i(m\phi + kr - \omega t)}{r} \tag{2.47}$$

2) The magnetic field is given by $\vec{B} = B_0 \hat{z} = B_0 \hat{r}$. As shown earlier, the actual applied field needs to be described in terms of the spherical coordinate unit vectors which yielded,

$$\vec{B} = B_0 \hat{z} = B_0 (\cos\theta \hat{r} - \sin\theta \hat{\theta}) \tag{2.48}$$

Therefore, the next part of the analysis will be to correct for the first assumption.

This time we utilize the expansion of equation (2.13) for $\vec{B} = B_0 \hat{z} = B_0 \hat{r}$ and $\boldsymbol{j}$ given by

$$\vec{j} = j_0 \frac{\exp i(m\phi + kr - \omega t)}{r} \tag{2.49}$$

Upon substitution yields

$$i\omega\vec{B} = \frac{1}{ne}\left\{B_0 \frac{\partial}{\partial r}\left(j\frac{\exp i(m\phi + kr - \omega t)}{r}\right)\right\} \tag{2.50}$$

Evaluating the derivative product gives

$$i\omega\vec{B} = \frac{B_0}{ne}\left(\frac{ik}{r} - \frac{1}{r^2}\right) j \exp i(m\phi + kr - \omega t) = \frac{B_0}{ne}\left(\frac{ik}{r} - \frac{1}{r^2}\right)\vec{j} \tag{2.51}$$

Substituting Maxwell's equation (2.8) for the current density ***j*** gives

$$\vec{B} = \frac{B_0}{i\mu_0\omega ne}\left(\frac{ik}{r} - \frac{1}{r^2}\right)\nabla\times\vec{B} \tag{2.52}$$

Taking the curl of both sides of equation (2.52) yields

$$\nabla\times\vec{B} = \left(\frac{B_0}{i\mu_0\omega ne}\right)\nabla\times\left\{\left(\frac{ik}{r} - \frac{1}{r^2}\right)\nabla\times\vec{B}\right\} \tag{2.53}$$

At this point, an analytical solution appears unlikely and the equation that will have to be numerically solved is

$$\alpha^2 k^2 r^2 \vec{B} + (ikr - 1)\nabla\times\left\{\left(\frac{ikr - 1}{r^2}\right)\nabla\times\vec{B}\right\} = 0 \tag{2.54}$$

The attempt of this analysis is similar to that in cylindrical coordinates. Understanding the plasma magnetic field structure showed when helicon waves could be supported. Therefore, the same approach was taking for analyzing a conical antenna, although ultimately the analysis became much more complex. At this juncture, the next step is to either numerical solve the equations involving spherical waves or to assume plane wave propagation in spherical coordinates subject to the conical wall boundary conditions which greatly simplifies the solution to the spherical harmonics obtained above.

IV. Hardware and Initial Setup

Current hardware consists of 3 quartz cylinders, each ~ 45 cm length. Two are straight cylinders with 3.81 cm and 6.35 cm diameters, while the last is a conical design starting at 3.81 cm diameter and ending at 10.16 cm diameter as shown schematically below in Figure 4.

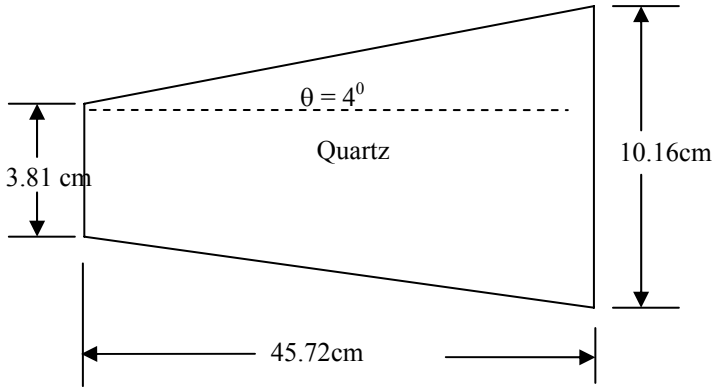

Figure 4. Schematic of conical quartz tube.

Each quartz tube is mounted through a conflat flange that is connected to a 0.5 m diameter, 1 m long cylindrical vacuum chamber that is pumped to a base pressure of $1x10^{-6}$ torr through a 250 l/s turbomolecular pump which is sufficient for helicon operation in the 10^{-4}-10^{-3} torr range. The pressure is monitored through a convectron gauge in the high pressure range (>10 mTorr) and by a cold cathode gauge in the low pressure range (< 10^{-4} torr). However, in the intermediary range of 10^{-4}-10^{-2} where neither gauge gives the most accurate pressure a capacitance manometer calibrated to this pressure range is used. Both vacuum chamber and quartz tube are mounted on a vibrationally insulated optics table.

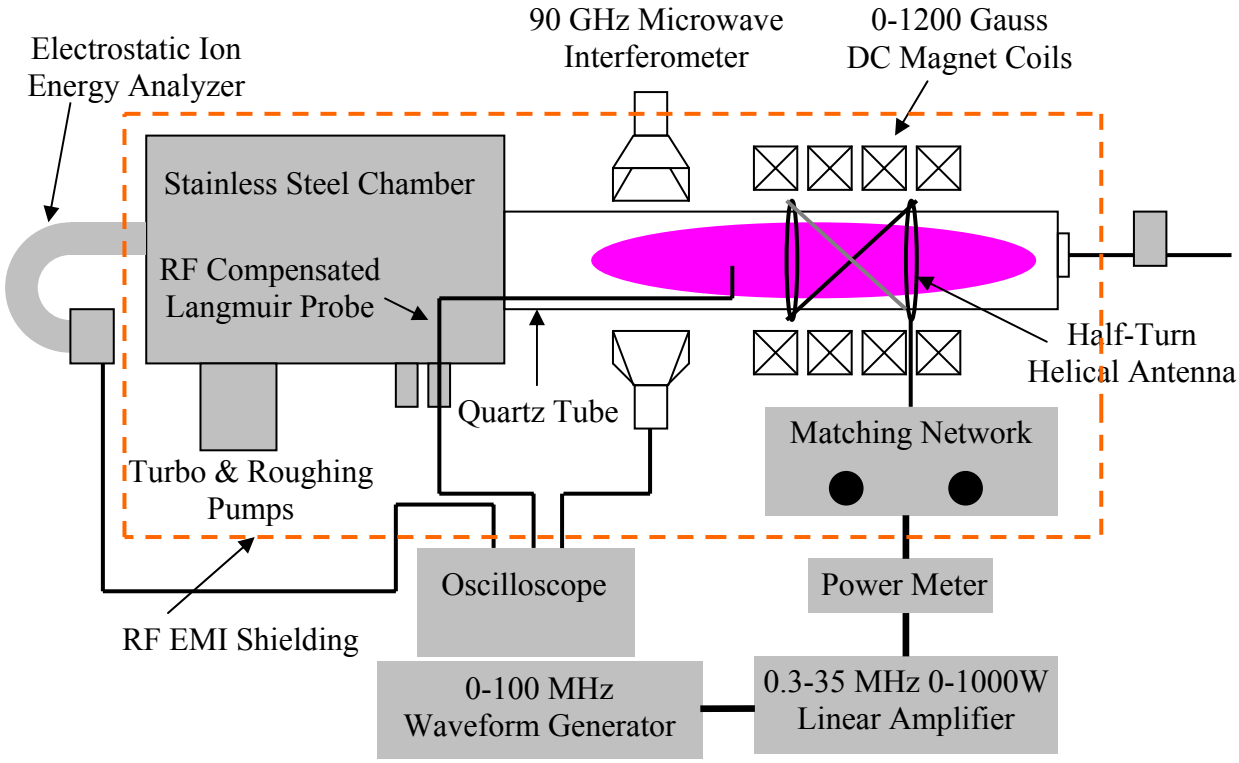

Figure 5. Schematic of AFRL Experimental Helicon research station.

Power to the antenna / plasma is supplied by a 0.3-35 MHz 1kW broadband RF generator fed through a autotune matching network to the *m=+1* helical antenna made of copper strap. The static magnetic field is supplied by 4 water-cooled magnets that can supply a continuous uniform field up to 1200 Gauss. A schematic of the current setup with chamber, magnets, antenna, matching network, and quartz tube are shown in

Current diagnostics consist of an RF compensated Langmuir probe with a copper compensation electrode and 4 chokes near the probe tip to minimize RF pickup at the driving frequency of 13.56 MHz and its first harmonic 27.12 MHz. The probe design was modeled after that of Sudit and Chen [28]. Similar to previous helicon work, a 90 GHz microwave interferometer has been used. Both diagnostics are currently ready for use upon proper RF shielding of interference.

Lastly, photos of the discharge have been taken to demonstrate the capability of generating RF and helicon discharges. Photos of inductively coupled plasma are shown below in Figure 6 for no applied external magnetic field.

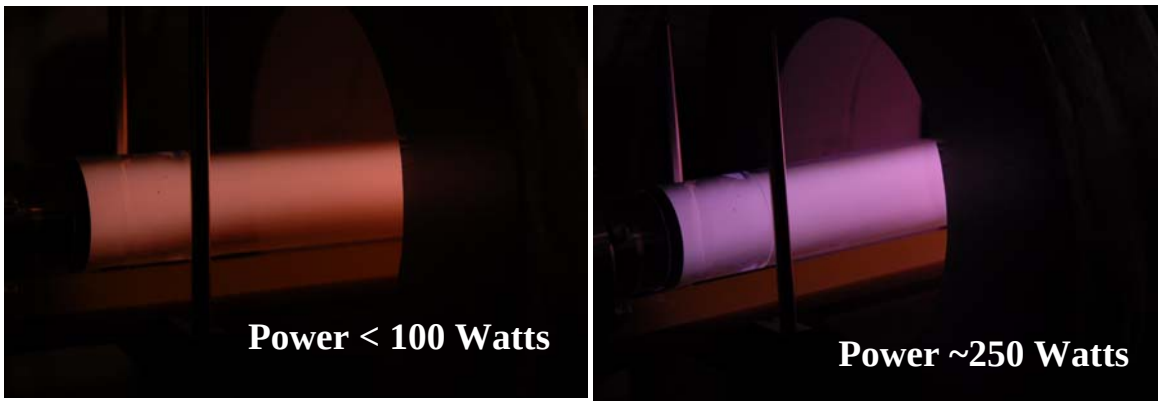

Figure 6. Plasma generated with *m=+1* antenna with no applied external B-field.

Photos for what is believed to be a helicon discharge at two different power levels and 800 gauss of external field are shown in Figure 7.

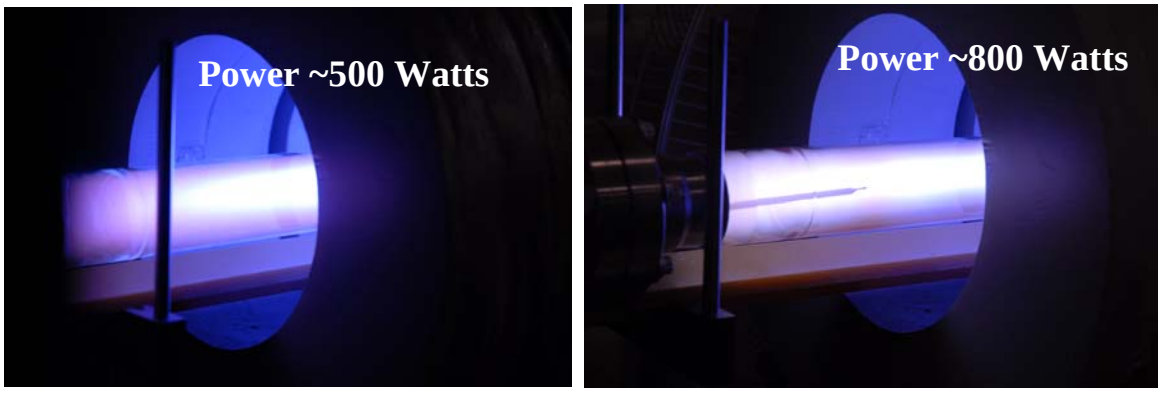

Figure 7. Plasma generated with *m=+1* antenna with 800 Gauss applied field.

V. Conclusions and Future Work

This study has revealed the fact that cylindrical geometry inherently simplifies the analysis toward arriving at the helicon dispersion relation and evaluating the wave structure as opposed to a different geometry such as a conical antenna analyzed with spherical coordinates. This is evident by the planar wave propagation in cylindrical geometry and the analysis is complicated by spherical wave propagation and the requirement of conservation of energy. However, the analysis has led to a differential equation that should be straightforward to analyze numerically and ultimately this is the next step. The goal of solving in spherical coordinates is to determine the wave structure and then compare the solution to that of the cylindrical helicon. The numerical and analytical aspect of this will be complemented with experimental measurements using b-dot probes to look at the radial fields.

The projected work will include comparisons between the three quartz tubes currently available, two cylinders of different radii and the conical tube. To date, the author is not aware that anyone has attempted a conical configuration for the antenna and insulating wall for plasma wave propagation. Based on a separate uniform density model, we arrived at the simple expectation that a smaller radius tube will yield higher density plasma for the same power, magnetic field, pressure, and frequency. Consequently, comparisons between the three quartz tubes as far as axial and radial density and temperature profiles will be done through the use of RF compensated Langmuir probe analysis verified against microwave interferometry data. The above measurements will have to be taken for different power levels and magnetic field configurations to determine the initiation of the helicon wave discharge as described in Section II.

Later on in this study, attention will be given to the observation of a double layer by Charles at fields of 250 gauss [29-31], as well as the effect of pressure on plasma potential from the antenna downstream. The majority of current helicon plasma operate at pressures > 1 mTorr where the mean free path for collisions is much less than the antenna and radii dimensions. However, as pointed out by Charles, at lower pressures (0.2-0.4 mTorr) the mean free path can be increased to the order of device dimensions and this is believed to be what allows the formation of the double layer. Therefore, the importance of investigating the pressure effects to determine whether this is the case should be explored.

References

1. Aigrain, P., *Les 'helicons' dans les semiconducteurs.* Proceedings of the International Conference on Semiconductor Physics, Prague, 1960.
2. Storey, L.R.O., *An Investigation of Whistling Atmospherics.* Philosophical Transactions of the Royal Society of London. Series A, Mathematical and Physical Sciences, 1953. **246**(908): p. 30.
3. Chen, F.F., *Plasma Ionization by Helicon Waves.* Plasma Physics and Controlled Fusion, 1991. **33**(4): p. 26.
4. Libchaber, A. and R. Veilex, *Wave Propagation in a Gyromagnetic Solid Conductor: Helicon Waves.* Physical Review, 1962. **127**(3): p. 3.
5. Rose, F.E., T. Taylor, and R. Bowers, *Low-Frequency Magneto-Plasma Resonances in Sodium.* Physical Review Letters, 1962. **127**(4): p. 3.
6. Lehane, J.A. and P.C. Thonemann, *An experimental study of helicon wave propagation in a gaseous plasma.* Proceedings of the Physical Society 1965. **85**.
7. Kuckes, A.F., *Resonant Absorption of Electromagnetic Waves in a Non-Uniformly Magentized Plasma.* Plasma Physics, 1968. **10**: p. 14.
8. Nyack, C.A. and P.J. Christiansen, *Dispersion Relation of High Frequency Waves in a Beam-Plasma System.* Plasma Physics, 1975. **17**: p. 5.
9. Klozenberg, J.P., B. McNamara, and P.C. Thonemann, *The dispersion and attenuation of helicon waves in a uniform cylidrical plasma.* Journal Of Fluid Mechanics, 1965. **21**: p. 545-563.
10. Boswell, R.W., *A study of Waves in Gaseous Plasma*, in *School of Physical Sciences*. 1970, The Flinders University of South Australia.
11. Boswell, R.W., *Very Efficient Plasma Generation by Whistler Waves Near the Lower Hybrid Frequency.* Plasma Physics and Controlled Fusion, 1984. **26**(10): p. 16.

12. Boswell, R.W. and D. Henry, *Pulsed high rate plasma etching with variable Si/SiO_2 selectivity and variable Si etch profiles.* Applied Physics Letters, 1985. **47**(10): p. 3.
13. Boswell, R.W. and R.K. Porteous, *Large volume, high density rf inductively coupled plasma.* Applied Physics Letters, 1987. **50**(17): p. 4.
14. Chen, F.F., *Nonlinear effects and anomalous transport in rf plasmas*, University of California, Los Angeles. p. 20.
15. Chen, F.F., *Introduction to Plasma Physics and Controlled Fusion*. Second ed. Vol. 1: Plasma Physics. 1984, UCLA: Plenum Press.
16. Chen, F.F., *Experiments on helicon plasma sources.* Journal of Vacuum Science and Technology: A, 1992. **10**(4): p. 13.
17. Chen, F.F., *Physics of helicon discharges.* Physics of Plasmas, 1996. **3**(5): p. 11.
18. Chen, F.F. and R.W. Boswell, *Helicons-The Past Decade.* IEEE Transactions on Plasma Science, 1997. **25**(6): p. 13.
19. Chen, F.F., M.J. Hsieh, and M. Light, *Helicon waves in non-uniform plasma.* Plasma Sources Science and Technology, 1994. **3**: p. 9.
20. Light, M. and F.F. Chen, *Helicon wave excitation with helical antennas.* Physics of Plasmas, 1995. **2**(4): p. 10.
21. Light, M., F.F. Chen, and P.L. Colestock, *Quiescent and unstable regimes of a helicon plasma.* Plasma Sources Science and Technology, 2002. **11**: p. 6.
22. Light, M., et al., *Axial propagation of helicon waves.* Physics of Plasmas, 1995. **2**(11): p. 10.
23. Miljak, D.G. and F.F. Chen, *Helicon wave excitation with rotating antenna fields.* Plasma Sources Science and Technology, 1998. **7**: p. 14.
24. Arnush, D. and A. Peskoff, *Helicon waves in a flaring magnetic field.* Plasma Physics and Controlled Fusion, 1995. **38**: p. 25.
25. Blackwell, D.D. and F.F. Chen, *2D Imaging of a Helicon Discharge*. 1997, University of California, Los Angeles, Electrical Engineering Department: Los Angeles. p. 17.
26. Chen, F.F., I.D. Sudit, and M. Light, *Downstream physics of the helicon discharge.* Plasma Sources Science and Technology, 1996. **5**: p. 8.
27. Sudit, I.D. and F.F. Chen, *Discharge equilibrium of a helicon plasma.* Plasma Sources Science and Technology, 1995. **5**: p. 11.
28. Sudit, I.D. and F.F. Chen, *RF compensated probes for high-density discharges.* Plasma Sources Science and Technology, 1994. **3**: p. 7.
29. Charles, C. and R.W. Boswell, *Laboratory evidence of a supersonics ion beam generated by a current-free "helicon" double layer.* Physics of Plasmas, 2004. **11**(4): p. 9.
30. Charles, C. and R. Bowell, *Current-free double-layer formation in a high-density helicon discharge.* Applied Physics Letters, 2003. **82**(9): p. 3.
31. Chavers, D.G., et al., *Status of Magnetic Nozzle and Plasma Detachment Experiment*, in *Space Technology and Applications International Forum*. 2006.

Effects of Helicon Wave Propagation Based on a Conical Antenna Design: Part I

Michael P. Reilly
Nuclear, Plasma, & Radiological Engineering
University of Illinois @ Urbana-Champaign

IEPC-2007-196

19 Sept 2007

Helicons: The Why?

- Well…everyone else is doing it…

Company/Institution	Research Time	Reference
AFRL	2006-Present	Personal Involvement
University of Illinois	2005-Present	Personal Involvement[28]
Starfire Industries	2005-Present	
NASA (Huntsville)	2006-Present	[29]
University of Washington	2004-Present	[30]
University of Texas	1998-Present	[31-36]
UCLA	1980's-Present	[3, 14-27]
University of Wisconsin	2003-Present	[37, 38]
Stanford University	2005-Present	
West Virginia University	2000-Present	[39, 40]
Cornell University	1991-???	[41]
Europe and Japan	2003?-Present	[42-44]
Australian National University	1965-Present	[10-13, 45-53]

Actually

- Electrode-less
- High Density at Low Power
  10^{19} m^{-3} @ 100's Watts
- High Ionization Efficiency > 90%
- Variable I_{SP} / Exhaust Velocity
- Wide range of gas / molecular propellant

What is a Helicon and Why?

- Subclass of Whistler Waves…what is a whistler wave?
  - Wave travels along magnetic field lines in free space
  - Right Hand Polarization
    - The electric field rotates clockwise when looking in the direction of propagation

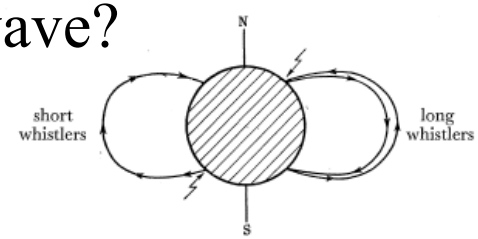

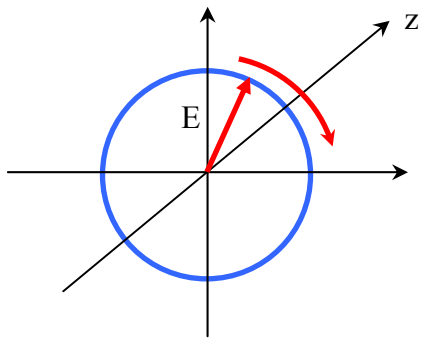

- Helicon Wave
  - Bounded whistler wave
  - Frequency between ion and electron gyro-frequency

Helicon Discharge

High Density, Axially Magnetized Plasma Column

$$\omega_{ci} \ll \omega_{LH} \ll \omega \ll \omega_{ce}$$

Argon

Helium

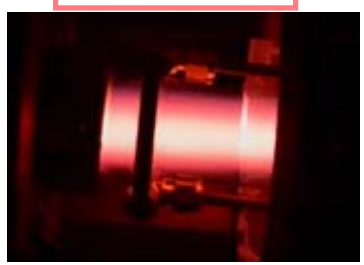

CCP, ICP, Helicon

- CCP – Capacitively Coupled Plasma
  - Electrons respond to E-Field → Gain Energy
  - Can ionize gas directly or indirectly
- ICP – Inductively Coupled Plasma
  - Time varying E-field generates a time varying magnetic field in the longitudinal direction
  - Induces azimuthal electric current → Gas breakdown
- Helicon Plasma
  - Breakdown is similar to ICP
  - Applied static B_0 allows radial and transverse waves
- Identifying the helicon mode
  - Often times done by looking for axial density "jumps"
    - Capacitive (E-mode) "pink"
      - Hollow Radial Density Profile
    - Inductive (H-mode) "purple"
      - Flat-Top Density Profile
    - Helicon (W-mode) "blue"
      - Sharply Peaked Core Density Profile
- More accurately identified by measuring the radial density profiles

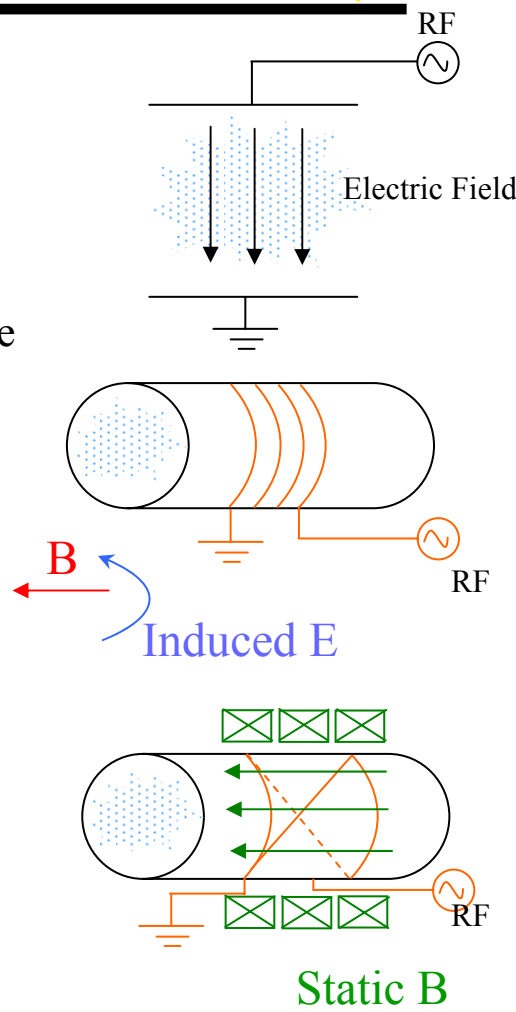

Cylindrical Helicon Theory (1)

Simplified Ohm's Law $ne\overline{E} = \overline{j} \times \overline{B}_0$

With perturbations $f \propto f_0 \exp i(m\theta + kz - \omega t)$

Result

$$\begin{cases} \overline{B} = \left(\dfrac{\omega}{k}\dfrac{\mu_0 e n_0}{B_0}\right)^{-1} \nabla \times \overline{B} \\ \nabla \times \overline{B} = \alpha \overline{B} \\ \nabla^2 \overline{B} + \alpha^2 \overline{B} = 0 \end{cases}$$

where $\alpha \equiv \dfrac{\omega}{k}\dfrac{\mu_0 e n_0}{B_0} = \dfrac{\omega}{k}\dfrac{\omega_p^2}{\omega_c c^2}$

$$\nabla \times \overline{E} = -\frac{\partial \overline{B}}{\partial t}$$
$$\nabla \times \overline{B} = \mu_0 \overline{j}$$
$$\nabla \cdot \overline{j} = 0$$
$$\nabla \cdot \overline{B} = 0$$
$$\nabla \times \nabla \times \overline{B} = \nabla(\nabla \cdot \overline{B}) - \nabla^2 \overline{B}$$
$$\nabla \times \nabla \times \overline{B} = -\nabla^2 \overline{B}$$

In cylindrical geometry for B_z $\quad B_z'' + \dfrac{1}{r}B_z' + \left(T^2 - \dfrac{m^2}{r^2}\right)B_z = 0$ $\quad$ where $T^2 = \alpha^2 + k^2$

Finite Solution at $r=0$ → $J_m(Tr)$

$$B_z = C_3 J_m(Tr) \qquad B_r = \frac{iC_3}{T^2}\left(\frac{m}{r}\alpha J_m - kJ_m'\right) \qquad B_\theta = \frac{C_3}{T^2}\left(\frac{m}{r}kJ_m + \alpha J_m'\right)$$

Apply Boundary Condition

Cylindrical Helicon Theory (2)

- Radial Current Density vanishes on the boundary

$j_r=0$ @ $r=a$

$$\nabla \times \bar{B} = \mu_0 \bar{j}$$

$$\mu_0 j_r = \frac{im}{r} B_z - ikB_\theta = 0$$

$$\nabla \times \bar{B} = \alpha \bar{B}$$

$$\frac{im}{r} B_z - ikB_\theta = \alpha B_r$$

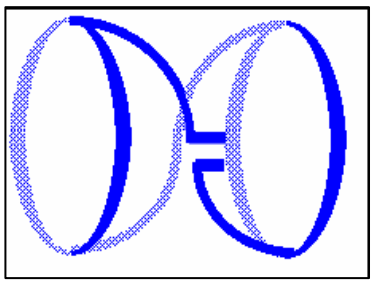

Helical Antenna

m = +1

$$B_r = \frac{iC_3}{T^2}\left(\frac{m}{r}\alpha J_m - kJ_m'\right)$$

$$m\alpha J_m(Ta) + kaJ_m'(Ta) = 0$$

Dispersion Relation for m=+1 Helicons

Uniform radial density profile

Cylindrical coordinates

$$\frac{B_0}{n_0} = \frac{e\mu_0 a}{Z_m}\frac{\omega}{k} \quad \rightarrow \quad \frac{3.83}{a} = \frac{\omega}{k}\frac{n_0 e\mu_0}{B_0}$$

Has been initial point for previous work

Internal Wave Structure

	r= 5 cm	r= 10 cm	r= 15 cm
B = 100 Gauss	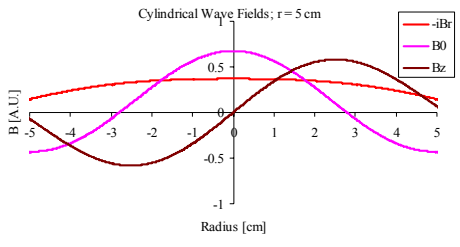	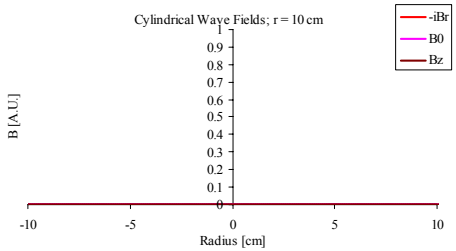	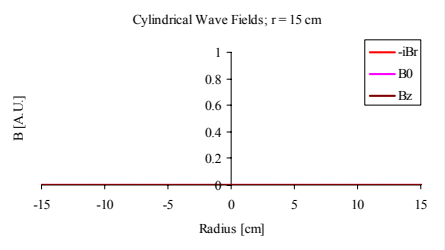
B = 250 Gauss	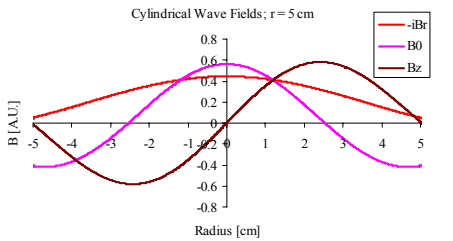	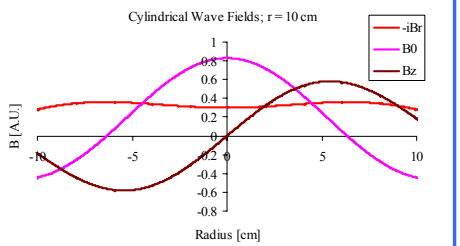	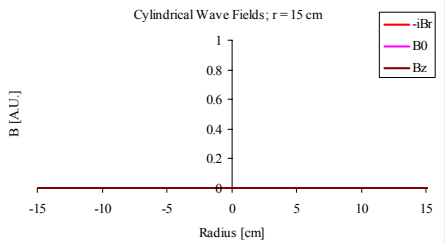
B = 500 Gauss	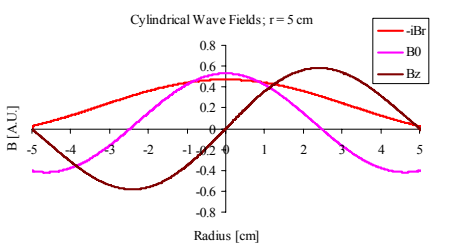	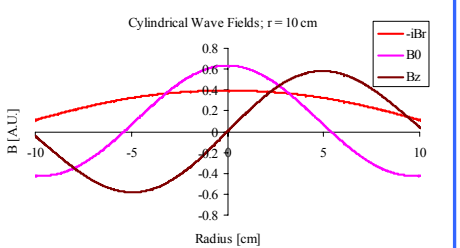	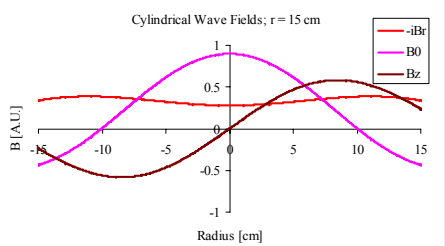
B = 1000 Gauss	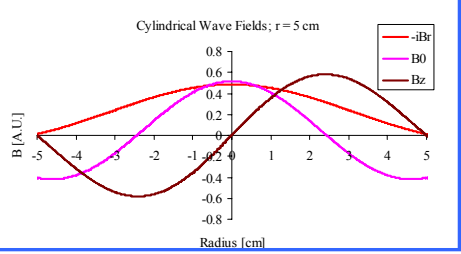	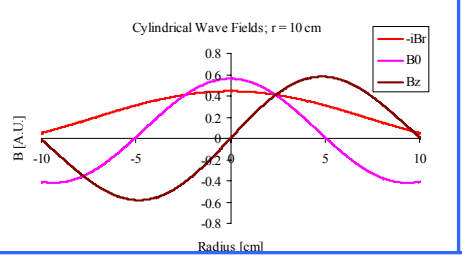	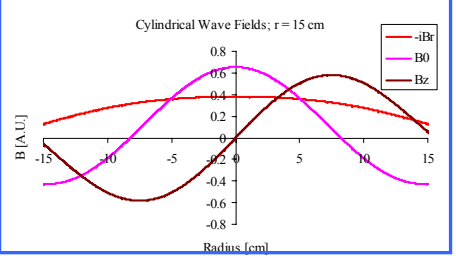

Transition to spherical

Cylindrical

$$f_0 \exp i(m\theta + kz - \omega t)$$

Uniform radial density

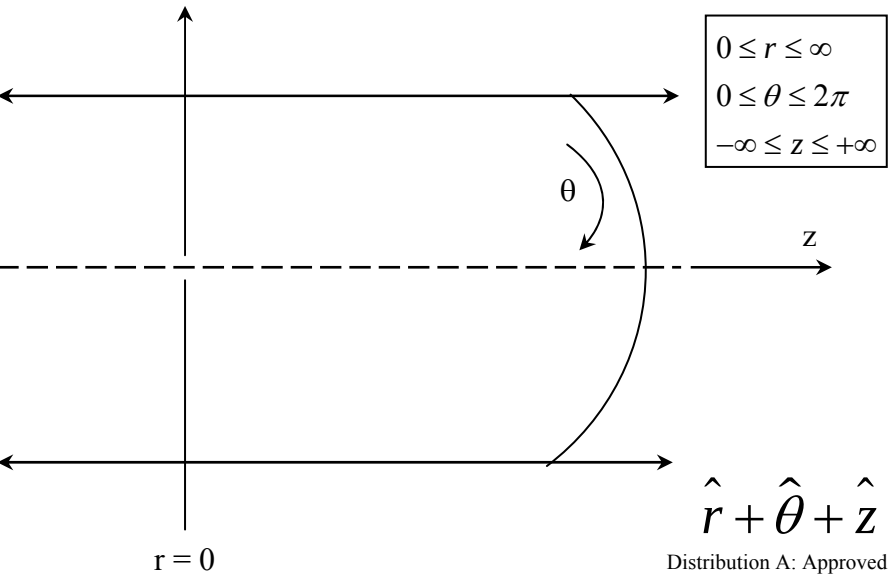

Spherical

$$f_0 \exp i(m\phi + kr - \omega t) \quad \text{vs.} \quad f_0 \frac{\exp i(m\phi + kr - \omega t)}{r}$$

Assumes no perturbation in θ direction

Waves travel at a constant radius '***r***'

$$\theta = \theta_{wall}$$

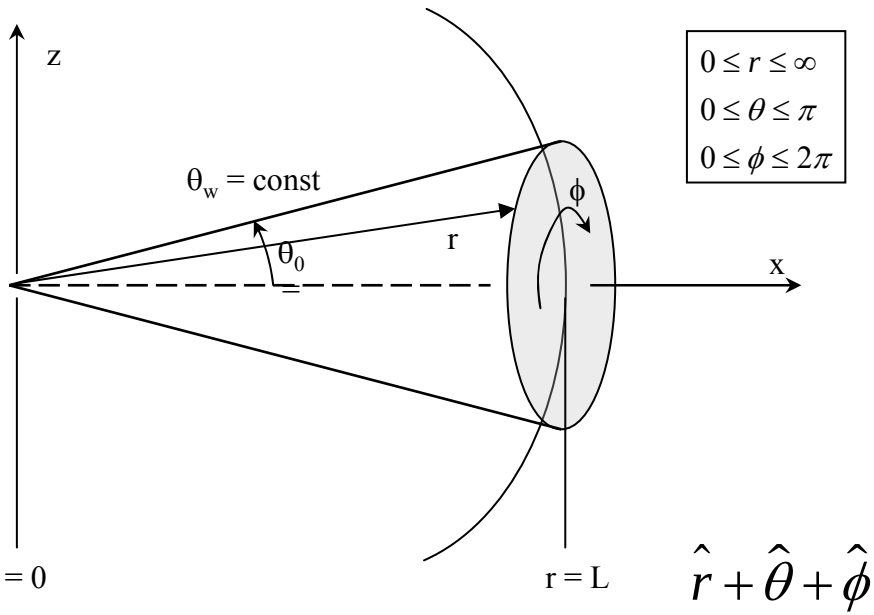

Spherical Waves (1)

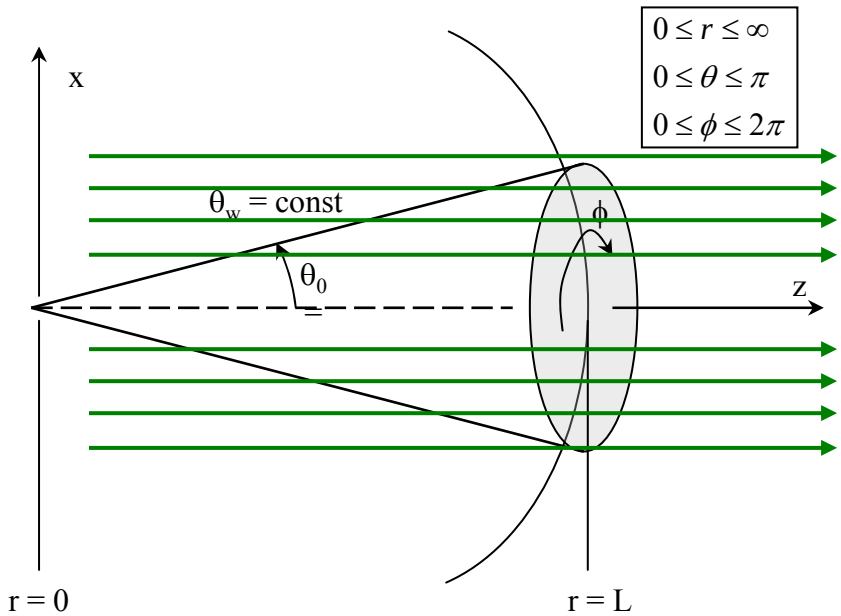

$$\vec{B} = B_0 \hat{z} = B_0(\cos\theta \hat{r} - \sin\theta\hat{\theta})$$

$$\vec{B} = B_0 \hat{z} = B_0 \hat{r}$$

$$\alpha \nabla \times \vec{B} = \nabla \times \left\{ (\cos\theta) \nabla \times \vec{B} \right\}$$

$$\vec{j} = j_0 \frac{\exp i(m\phi + kr - \omega t)}{r}$$

- Complex solution
- Requires numerical analysis

Spherical Waves (2)

$$f_0 \exp i(m\phi + kr - \omega t) \quad \text{vs.} \quad f_0 \frac{\exp i(m\phi + kr - \omega t)}{r}$$

- Separable in Spherical Coordinates

$$\frac{1}{r^2}\frac{\partial}{\partial r}\left(r^2 \frac{\partial \vec{B}}{\partial r}\right) + \frac{1}{r^2 \sin\theta}\frac{\partial}{\partial \theta}\left(\sin\theta \frac{\partial \vec{B}}{\partial \theta}\right) + \frac{1}{r^2 \sin^2\theta}\frac{\partial^2 \vec{B}}{\partial \phi^2} + \alpha^2 \vec{B} = 0$$

$$B(r,\theta,\phi) = R(r)\Theta(\theta)\Phi(\phi)$$

$$B(r,\theta,\phi) = \sum_{l=0}^{\infty}\sum_{m=-l}^{l} a_{lm} j_l(\alpha r) Y_l^m(\theta,\phi)$$

- Planar Waves vs. Spherical Waves

$$\alpha^2 k^2 r^2 \vec{B} + (ikr - 1)\nabla \times \left\{\left(\frac{ikr - 1}{r^2}\right)\nabla \times \vec{B}\right\} = 0$$

Why 4 degree angle

- Comparison between cylindrical tubes and conical
- Investigate wave field structure
- Density/Temperature/Potential results for same operating parameters

- Small angle approximates B field with $\hat{r}$ direction

- Tubes in use
  - 3.81 cm diameter cylinder
  - 6.35 cm diameter cylinder
  - Conical design →

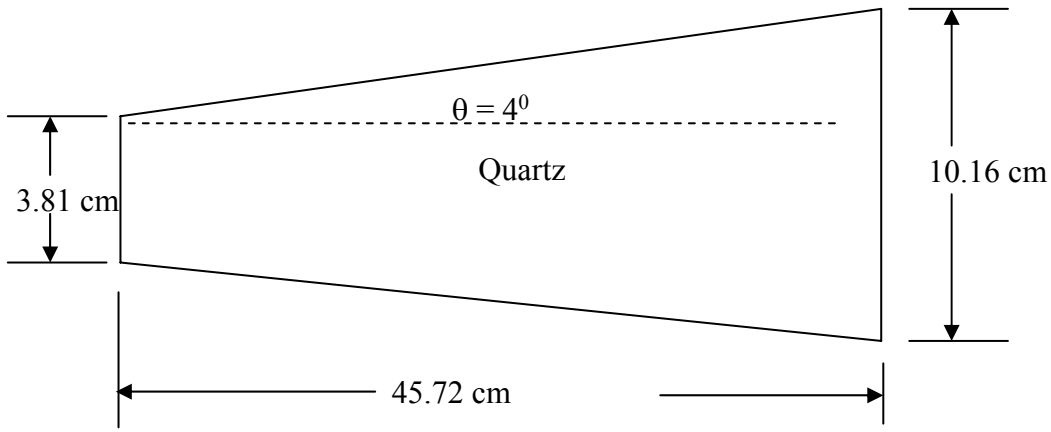

Setup Schematic

- Laboratory Parameters
  - Power = 0-5 kW
  - B-field = 0-2 kGauss
  - Pressure = 0.2-20 mTorr
  - Radius = 1-15 cm
  - Frequency = 0.5-27.12 MHz
  - Antenna length = 5-30 cm
  - Gas = H_2,He,Ar,Xe

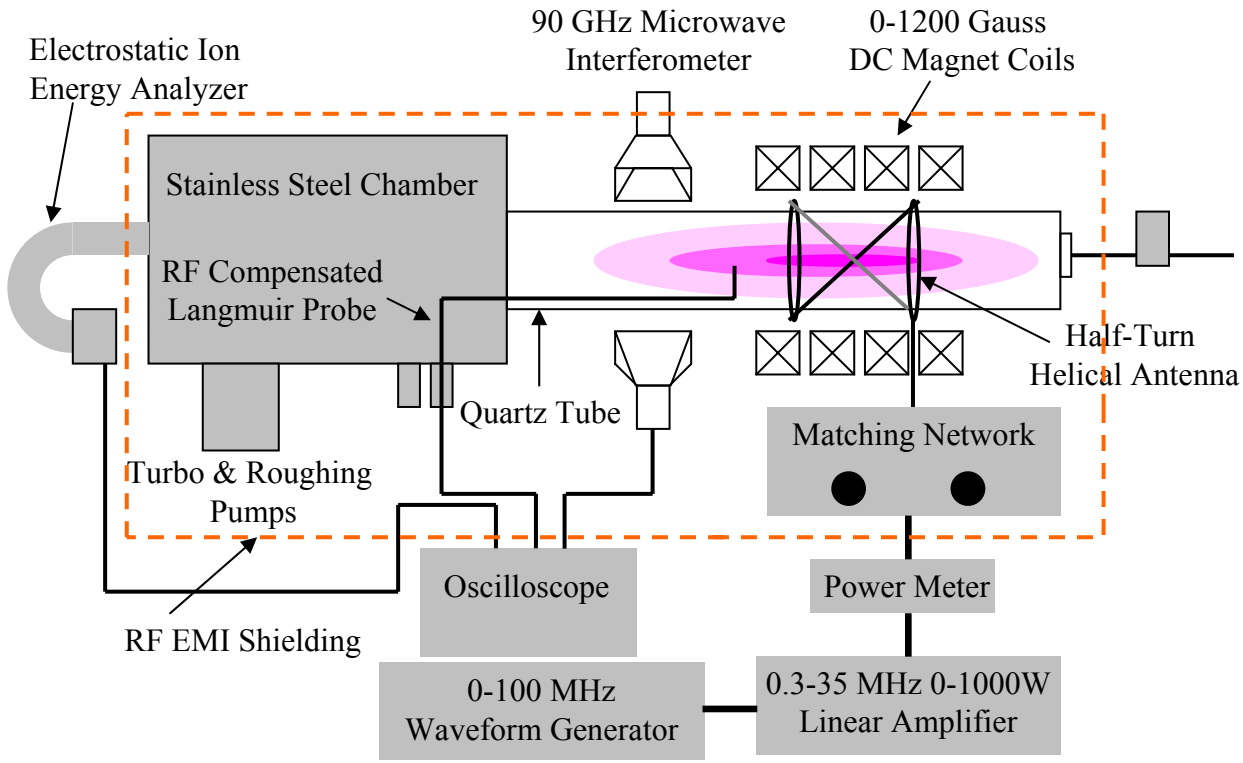

Argon Discharge Photos

- No Applied B-field

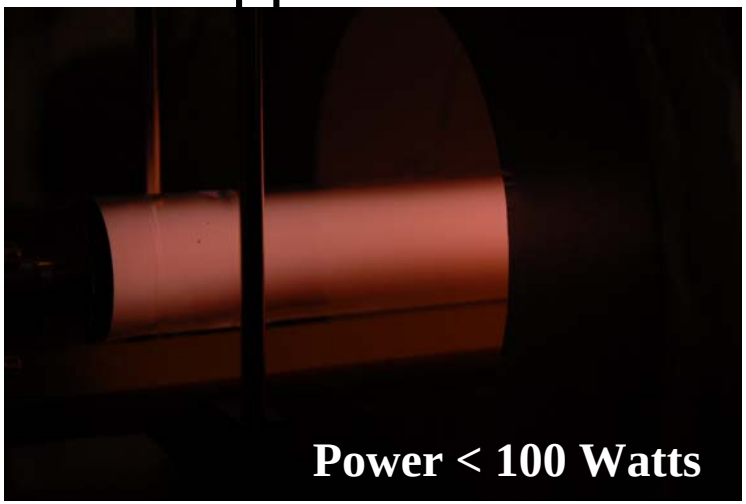

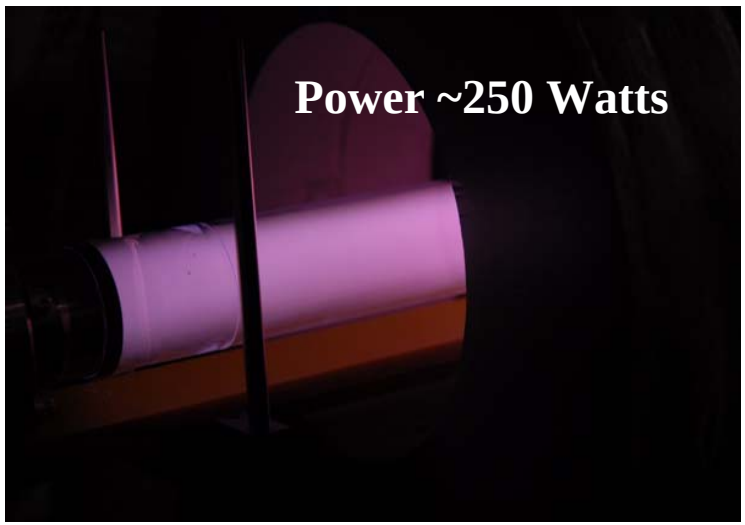

- High B-field ~ 1kGauss

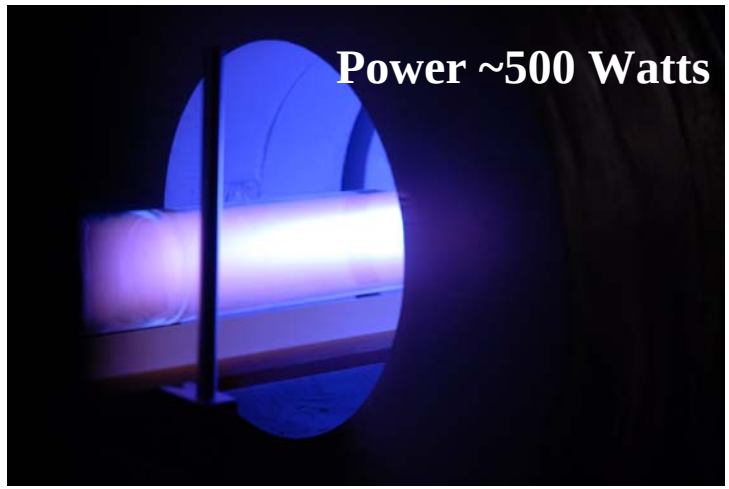

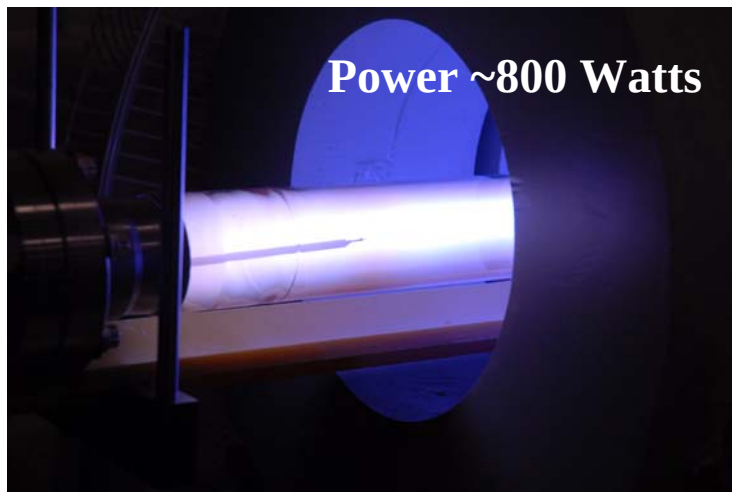

Summary and Conclusion

- Dispersion relations which lead to geometry considerations
- Results for infinite homogeneous plasma shown lower hybrid frequency waves with 1kGauss B-field in agreement with a few experimental data points.
- Effects can be enhanced at low pressure and through control of RF wave absorption

Questions ?